Proc. of the 5th WSEAS/IASME Int. Conf. on Electric Power Systems, High Voltages, Electric Machines, Tenerife, Spain, December 16-18, 2005 (pp143-148)

Control Methods for Doubly-Fed Reluctance Machines

MILUTIN JOVANOVIĆ and KRISHNA BUSAWON

School of Computing, Engineering and Information Sciences
University of Northumbria at Newcastle
Newcastle upon Tyne NE1 8ST
United Kingdom
milutin.jovanovic@unn.ac.uk

Abstract:- The paper considers aspects of scalar V/f control, vector control and direct torque (and flux) control (DTC) of an emerging cost-effective technology for limited speed range applications - the brushless doubly fed reluctance machine (BDFRM). Apart from giving a comprehensive review of the various control methods, its major contribution is the presentation and experimental verification of a sensorless DTC scheme which, unlike most of the existing algorithms, can perform well down to zero supply frequency of the inverter-fed winding.

Key-Words:- Control, Brushless, Doubly-Fed, Reluctance Machines, Slip Power Recovery.

1 Introduction

The inverter-fed brushless doubly fed reluctance machine (BDFRM) is an attractive candidate for variable speed applications due to its low cost, high reliability and lower harmonic injection into the supply mains. The economic benefits and improved power quality of the BDFRM drive can be attributed to the machine's slip power recovery property allowing the use of a smaller inverter (relative to the machine rating), and especially in systems with limited speed ranges (such as pumps and wind turbines [1]) where the inverter size and cost can be further reduced. Other important advantages of the BDFRM over conventional singly-excited machines include the operational mode flexibility (it can operate as an induction machine in case of the inverter breakdown, or as a classical wound rotor synchronous machine with field control), the wider speed ranges afforded by sub-synchronous and super-synchronous operation in both motoring and generating regimes, and the inherently decoupled control of torque and power factor [2], efficiency [1] or any other performance parameter of interest [3]. The latter feature implies the relative control simplicity as additional decoupling mechanisms are not required.

When compared with machines of similar properties, the conventional doubly-excited wound rotor induction machine (DEWRIM) or the closely related, brushless doubly-fed induction machine (BDFIM), the BDFRM is superior in many respects. The absence of brush gear and slip rings is an obvious advantage over the DEWRIM particularly for off-shore wind generators requiring high reliability and low maintenance. On the other hand, the possibility of using a cageless synchronous reluctance (SyncRel) rotor makes it more efficient, more mechanically robust and much easier to control than the BDFIM having a special 'nested' cage rotor construction [4]. It has been shown that with increasing saliency-ratio of the rotor, the BDFRM overall performance improves as it does with the Syncrel [5]. This fact is important as the recent technological advances in the development of modern Syncrel rotors are directly applicable to the BDFRM.

The paper gives a thorough review of the main control methods for the BDFRM. While the material to be presented is not new, it is comprehensive in nature and can serve as a good reference for research on the BDFRM. Algorithms for scalar control and direct torque (and flux) control (DTC) are proposed and examined by computer simulations and experimentally. Vector control principles are only briefly discussed for entity of analysis, and because a field-oriented control scheme, similar to the one considered in this paper, has already been experimentally validated in [3]. In terms of the DTC, the paper largely builds upon the recently published work of the author and his colleagues [6, 7]. The practical verification of the simulation studies carried out in [6] has been achieved in [7], but the respective DTC scheme could not provide satisfactory transient response from the machine to the speed changes. This limitation has been overcome in the meantime, and a new set of experimental results showing the improved dynamic performance of the machine is presented in this paper.

2 Dynamic Models

The space-vector voltage and flux equations for the machine in a stationary reference frame using standard

notation and assuming motoring convention are as follows [8]:

$$\underline{u}_{p_s} = R_p \underline{i}_{p_s} + \frac{d\underline{\lambda}_{p_s}}{dt} = R_p \underline{i}_{p_s} + \left.\frac{d\underline{\lambda}_{p_s}}{dt}\right|_{\theta_p \text{ const}} + j\omega_p \underline{\lambda}_{p_s} \tag{1}$$

$$\underline{u}_{s_s} = R_s \underline{i}_{s_s} + \frac{d\underline{\lambda}_{s_s}}{dt} = R_s \underline{i}_{s_s} + \left.\frac{d\underline{\lambda}_{s_s}}{dt}\right|_{\theta_s \text{ const}} + j\omega_s \underline{\lambda}_{s_s} \tag{2}$$

$$\underline{\lambda}_{p_s} = L_p \underline{i}_{p_s} + L_{ps} \underline{i}^*_{s_s} e^{j\theta_r} \tag{3}$$

$$\underline{\lambda}_{s_s} = L_s \underline{i}_{s_s} + L_{ps} \underline{i}^*_{p_s} e^{j\theta_r} \tag{4}$$

where the subscripts 'p' and 's' denote the primary (grid-connected) and secondary (inverter-fed) winding quantities respectively. By omitting the exponential terms in (3)-(4), one obtains the rotating frame equivalents of (1)-(4) which, in a primary flux oriented control form ($\lambda_{pq} = 0$), become:

$$\underline{u}_p = R_p \underline{i}_p + \frac{d\lambda_p}{dt} + j\omega_p \lambda_p \tag{5}$$

$$\underline{u}_s = R_s \underline{i}_s + \frac{d\underline{\lambda}_s}{dt} + j\omega_s \underline{\lambda}_s \tag{6}$$

$$\lambda_p = L_p \underline{i}_p + L_{ps} \underline{i}^*_s \tag{7}$$

$$\underline{\lambda}_s = L_s \underline{i}_s + L_{ps} \underline{i}^*_p = \sigma L_s \underline{i}_s + \underbrace{\frac{L_{ps}}{L_p} \lambda_p}_{\lambda_{ps}} \tag{8}$$

where $\sigma = 1 - L_{ps}^2/(L_p L_s) = 1 - k_{ps}^2$ is the leakage factor (defined as with an induction machine), $k_{ps} = L_{ps}/\sqrt{L_p L_s}$ is the coupling coefficient between the windings (as in a power transformer), $L_{p,s,ps}$ are the respective 3-phase inductances [5, 8] and λ_{ps} is the primary flux linking the secondary winding i.e. the mutual flux (Fig. 1).

From the fundamental BDFRM theory [8], one can establish the following condition for the machine torque production:

$$\omega_r = p_r \omega_{rm} = \omega_p + \omega_s \Longleftrightarrow \theta_r = p_r \theta_{rm} = \theta_p + \theta_s \tag{9}$$

where $\omega_{rm} = d\theta_{rm}/dt$ is the rotor mechanical angular velocity, p_r is the number of rotor poles, $\omega_{p,s} = d\theta_{p,s}/dt$ are the applied angular frequencies to the windings[1], and $\theta_{r,p,s}$ are the corresponding reference frame positions as illustrated in Fig. 1 (the rotor frame is omitted for convenience). Notice that $\omega_s > 0$ for 'super-synchronous' ($\omega_{rm} > \omega_{syn}$) and $\omega_s < 0$ for 'sub-synchronous' ($\omega_{rm} < \omega_{syn}$) machine operation[2].

[1]The supply frequencies and pole numbers are different with the reluctance rotor having half the total number of stator poles to provide rotor position dependent magnetic coupling between the windings and torque production from the machine.

[2]The BDFRM synchronous speed is defined as $\omega_{syn} = \omega_p/p_r$ and occurs with the DC secondary winding i.e. when $\omega_s = 0$. The 'negative' secondary frequency at sub-synchronous speeds simply means the opposite phase sequence of the secondary to the primary winding.

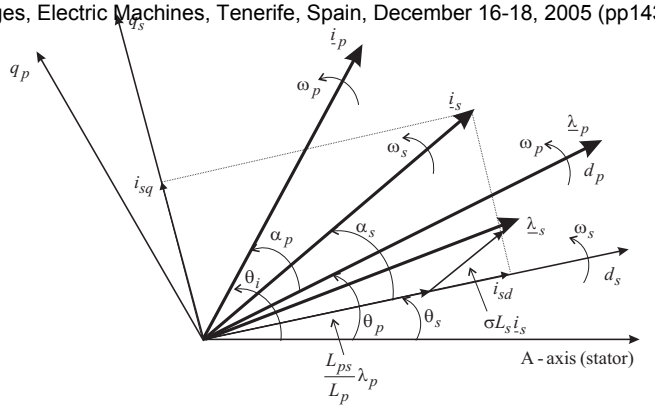

Figure 1: Reference frames and characteristic phasors

It should be emphasised that the primary and secondary equations above are in two different reference frames, $d_p q_p$ and $d_s q_s$, rotating at ω_p and $\omega_s = \omega_r - \omega_p$ respectively. If one arbitrary chooses the $d_p q_p$ frame to be aligned with the primary flux vector λ_p (since this is of fixed frequency and approximately constant magnitude due to the winding grid connection), then the $d_s q_s$ frame lies along the mutual flux vector λ_{ps} as in Fig. 1. The secondary flux vector, λ_s, and λ_{ps} are then stationary one with respect to the other (they both rotate at ω_s), and for the machine to produce average torque there must be a phase shift between them as will be formulated later in the DTC section.

3 Scalar Control

In pump-type applications simple scalar control is quite a satisfactory solution as fast dynamics of a machine is not required and steady-state performance only matters. Furthermore, speed ranges and related frequency variations in these systems are usually limited which alleviate stability problems commonly associated with this method. Some preliminary Simulink® results obtained by performing the V/f=const control as in Fig. 2 are shown in Fig. 3. The proposed scalar control strategy is by no means optimal and has been developed by analogy to the cage induction machine case. The supply voltage boost, normally present with the induction machines to compensate for resistive voltage drops and increase torque at lower speeds, is not implemented here for convenience of analysis.

The BDFRM has been started as a slip ring induction machine (with the shorted secondary winding) close to the synchronous speed (750-rpm) when the inverter is connected and the control enabled. Such a starting procedure is desirable to prevent the current overloading of the fractionally-rated inverter during start-up. It can be seen that the machine response to speed and/or load torque step changes is expectedly faster and smoother under closed-loop control. This performance improvement is a consequence of the 'stabilising' action of the PI block in Fig. 2. The machine oscillatory behavior

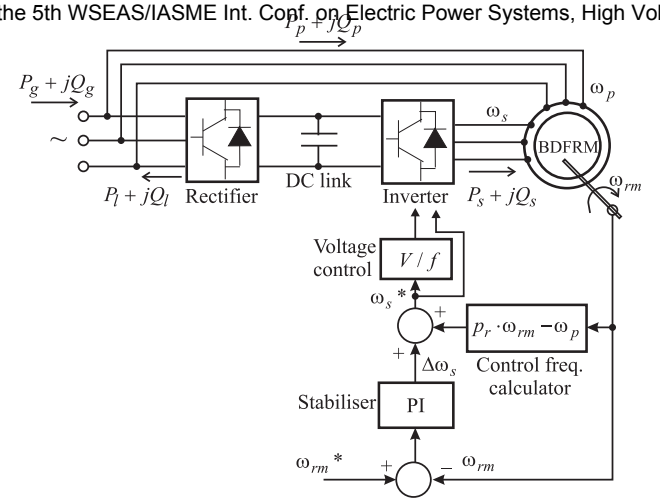

Figure 2: The BDFRM drive with scalar control

without the speed feedback is evident from the speed waveform but is still within stability margins. However, for larger step changes in the command speed (and hence the secondary frequency), the oscillations would get magnified and undamped leading to instability.

4 Vector Control

One of the most important advantages of the BDFRM is the inherently decoupled control of torque and primary winding (line) reactive power. Substituting for (5)-(8) into the general expression for complex electrical power – $P_p + jQ_p = \frac{3}{2}(\underline{u}_p \underline{i}_p^* + \underline{u}_s \underline{i}_s^*)$, one can derive the expressions for the secondary real power (P_s), electromagnetic torque (T_e) and primary reactive power (Q_p) in a primary flux oriented control form [3, 8]:

$$P_s = \frac{\omega_s}{\omega_p + \omega_s} P_{out} = \frac{\omega_s}{\omega_p} P_p \tag{10}$$

$$T_e = \frac{P_{out}}{\omega_{rm}} = \frac{3}{2} p_r \frac{L_{ps}}{L_p} \lambda_p i_{sq} \tag{11}$$

$$Q_p = \frac{3}{2} \frac{\omega_p \lambda_p}{L_p} (\lambda_p - L_{ps} i_{sd}) \tag{12}$$

As can be seen from (11) and (12), T_e is controlled by the secondary q-axis current, i_{sq}, and Q_p by the secondary d-axis current, i_{sd}, and there is no coupling between the two expressions (since λ_p is virtually constant). The maximum torque per secondary ampere (MTPSA) allows the minimum current loading of the supply inverter for a given torque if $i_{sd} = 0$ i.e. $i_s = i_{sq}$ [2, 5]. Other benefits of this control strategy are the lower copper losses and consequently higher efficiency of the machine. Note also that the machine slip power recovery property is hidden in (10). For example, if the secondary is supplied at the line frequency (i.e. $\omega_s = \omega_p$), the inverter has to handle at most half the output power. However, if $\omega_s = 0.25\omega_p$, then the secondary winding contribution to the machine power

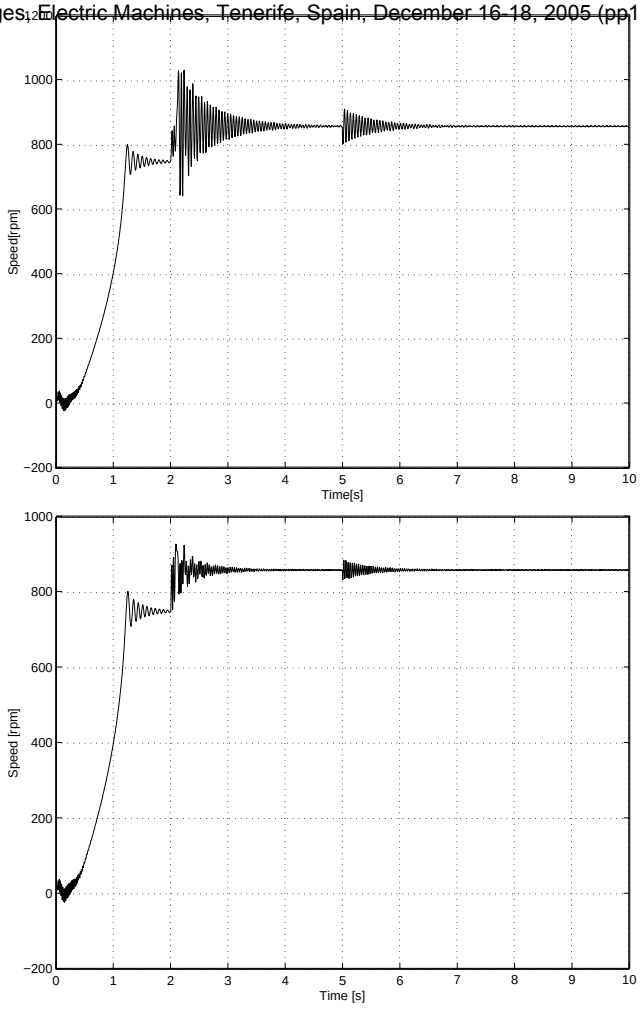

Figure 3: BDFRM speed with open-loop (top) and closed-loop (bottom) V/f control for desired speed and load torque step changes at 2-s and 5-s, respectively)

production is only 20%. Therefore, in applications where the BDFRM is required to operate in a narrow range around synchronous speed where ω_s values are small, a partially-rated inverter can be used.

Q_p is regulated by the amount of flux that is being produced in the primary via the mutual coupling from the secondary which corresponds to the $L_{ps}\underline{i}_s^*$ term in (7). If necessary, the secondary can supply all the flux required for the machine magnetization (by keeping $i_{sd} = \lambda_p / L_{ps}$), and in this case Q_p becomes zero i.e. the primary power factor is then unity. However, a larger inverter would be needed to accommodate this [2].

If supplied from a dual-bridge PWM converter, the BDFRM can operate as an efficient reactive power compensator since it is possible to minimise total copper losses in the machine for a given torque by appropriately controlling i_{sd} and hence Q_p according to (12) [2]. The unity (or even leading) line power factor can be achieved by supplying the primary reactive power not from the grid or the inverter (through the secondary winding) but using the PWM rectifier ($Q_g = 0$ and $Q_l = Q_p$ in Fig. 2). The other advantages of employing a bi-directional PWM converter are the real

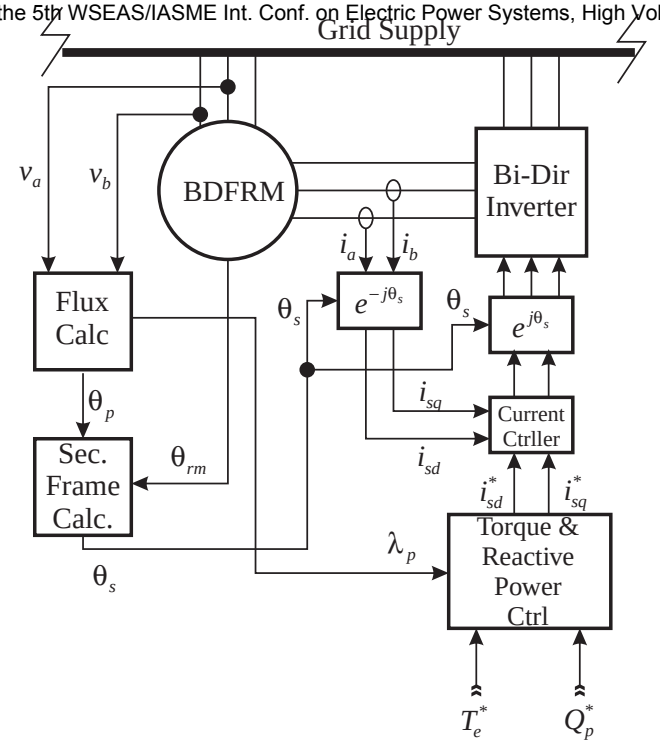

Figure 4: A simplified block diagram of the field-oriented torque controller for the BDFRM

power regenerating capability with DC link voltage stability, the four-quadrant operation and the lower line harmonic content (and therefore improved power quality).

The structure of a typical BDFRM drive with vector control based on (11) and (12) is presented in Fig. 4 [3]. Given that the secondary winding quantities are only controllable, one should first identify the secondary frame position (θ_s) using (9). The rotor position, θ_{rm}, is usually detected by a shaft sensor while the primary flux angle (Fig. 1), θ_p, can be estimated with very little error by integrating the measured grid voltages and neglecting the resistive voltage drop [3] using:

$$\underline{\lambda}_{p_s} = \lambda_p e^{j\theta_p} = \int \left(\underline{u}_{p_s} - R_p \underline{i}_{p_s}\right) dt \approx \int \underline{u}_{p_s} dt \tag{13}$$

Once θ_s is known one can implement current control of the secondary $d_s q_s$ components (and thus torque and primary reactive power) for a desired strategy [2, 5] in a conventional way as outlined in Fig. 4.

5 Direct Torque Control (DTC)

5.1 General Considerations

Since its original development for cage induction machines [9], the DTC concept, owing to its versatility and little machine parameter dependence, has been successfully used for torque and stator flux control of almost all brushless machines. However, its application to the BDFRM or BDFIM, has not yet been reported in the published literature by other researchers. It is well-known that most back-emf based control approaches, including DTC, suffer from low frequency stability problems due to flux estimation inaccuracies caused by unknown resistance variations at lower supply voltages. It is mainly for this reason that this control method has been extremely popular only for high-speed applications where the resistance effects are less pronounced. In this sense, the DTC appears not to be an appropriate control solution for BDFRM drives with limited variable speed capability, and therefore low secondary operating frequencies. Fortunately, these common DTC difficulties in the low frequency region can be overcome in the BDFRM as both its windings are accessible externally, which allows more freedom in parameter estimation and control. A conventional DTC algorithm for the cage induction machine [9, 10] can serve as a good starting point in the DTC development for the BDFRM. In fact, from a control point of view, the primary and secondary windings of the BDFRM play the roles of the rotor and stator windings of the induction machine respectively. This means that by analogy to the induction machine case the DTC variables for the BDFRM should be the secondary flux magnitude and torque.

5.2 Fundamental Principles

One of the key issues of the DTC application to the BDFRM is how to control the secondary flux so that the desired torque dynamics is achieved. An answer to this question can be found from (8) and a DTC form of (11):

$$\underline{\lambda}_s = \lambda_{sd} + j\lambda_{sq} = \sigma L_s i_{sd} + \frac{L_{ps}}{L_p}\lambda_p + j\sigma L_s i_{sq} \tag{14}$$

$$T_e = \frac{3p_r}{2\sigma L_s}\left|\underline{\lambda}_{ps} \times \underline{\lambda}_s\right| = \frac{3p_r}{2\sigma L_s}\frac{L_{ps}}{L_p}\lambda_p \lambda_s \sin\delta \tag{15}$$

It is evident from (14) and (11) that λ_{sq} is a torque producing secondary flux component since it is directly proportional to i_{sq}. Therefore an increase (decrease) of torque should result in the secondary flux angle in both the $d_s q_s$ frame (i.e. δ in the above torque expression) and the stationary frame (i.e. $\delta + \theta_s$ according to Fig. 1) to change accordingly i.e. to instantly increase(decrease). Consequently, there is no need to know the secondary frame position to be able to implement the DTC, and this can be done in a stator frame as usual for this method. A shaft position sensor shown in Fig.5 is only used for accurate speed detection for condition monitoring purposes, and not in the torque controller.

[3] In most cases, and especially with larger machines, this approximation is justified by the dominant back-emf values at line frequency.

At super-synchronous speeds both the d_sq_s and d_pq_p frames rotate in the same 'counter-clockwise' direction, and one can use the look-up table of optimal inverter switchings similar to cage induction machines [9, 10]. If the BDFRM is operated in the sub-synchronous mode, then the look-up table for 'clockwise' rotation should be applied. Note, however, that unlike the induction machine, the BDFRM speed in the latter case is still positive (and so is the torque reference) i.e. in 'anti-clockwise' direction but the d_sq_s frame now rotates 'clockwise' (due to the opposite phase sequence of the secondary winding to the primary), which is indicated by $\omega_s < 0$ in (9). In this speed region, the secondary supply voltage will simply reverse its polarity to allow power regeneration through the secondary winding for the machine operating as a motor[4] as follows from (10) for $\omega_s < 0$. The relative positions of the secondary flux and mutual flux phasors should remain unchanged according to (15) so that 'motoring' torque (acting 'anti-clockwise') is produced by the machine.

The main reason for using different look-up tables in super- and sub-synchronous modes is the ambiguous influence of the zero voltage vectors to the torque variations. If the active voltage vectors are only employed, then a single look-up table can do the job, in which case the speed dependence of the torque controller disappears as illustrated in Fig.5. The benefits and limitations of taking this approach have been elaborated in [6, 7] and won't be repeated here.

As discussed earlier, the use of (2) for estimating the secondary flux magnitude and stationary frame angle is not convenient at low secondary frequencies. However, considering that both the primary and secondary quantities are measurable in the BDFRM, the following alternative expression can be derived using (1), (3) and (4):

$$\underline{\lambda}_{s_s} = L_s \underline{i}_{s_s} + \underline{i}^*_{p_s} \frac{\underline{\lambda}_{p_s} - L_p \underline{i}_{p_s}}{\underline{i}^*_{s_s}} \qquad (16)$$

where $\underline{\lambda}_{p_s}$ is given by (13). This estimation technique obviously avoids voltage integration and associated problems but requires knowledge of the winding self inductances $L_{p,s}$ at the expense. The experimental results presented in the following section will demonstrate that despite the increased parameter dependence, the BDFRM can be successfully controlled down to zero secondary frequency (i.e. at synchronous speed) unlike other machines with DTC.

The torque estimate can be obtained using the following expression:

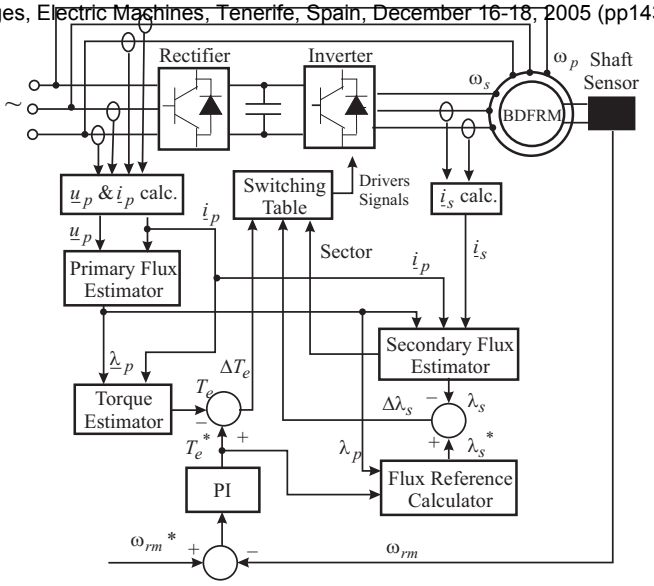

Figure 5: BDFRM drive with DTC

$$T_e = \frac{3}{2} p_r \left| \underline{\lambda}_{p_s} \times \underline{i}_{p_s} \right| = \frac{3}{2} p_r \lambda_p i_p \sin \measuredangle(\underline{\lambda}_{p_s}, \underline{i}_{p_s}) \qquad (17)$$

High estimation accuracy can be expected in practice as (17) is not only machine parameter independent but is also based on the primary quantities having 'clean' waveforms[5]. The primary flux magnitude and angle $\measuredangle(\underline{\lambda}_{p_s}, \underline{i}_{p_s}) = \alpha_p$ can be calculated from the grid voltage and primary current measurements using (13) and the fact that $\alpha_p = \theta_i - \theta_p$ where $\theta_{i,p}$ are the stationary frame angles of the primary current and flux phasors (Fig. 1).

5.3 Experimental Verification

The experimental results have been generated by executing the DTC scheme in Fig.5 on a small BDFRM prototype using dSPACE®. The machine parameters and other relevant details about the test system can be found in [6, 7]. The BDFRM is started with the shorted secondary terminals (as described in Section 3), and after reaching the steady-state, the control is enabled (this corresponds to 4-s time instant in the plots presented).

Fig.6 clearly demonstrates the BDFRM ability to operate successfully in a narrow range around, and even at synchronous speed (78.54 rad/s = 750 rpm) when the secondary frequency is zero (from about 16-s onward). It is evident that the BDFRM speed prior to the control activation is below synchronous as expected due to the presence of no-load losses (remember that the BDFRM emulates the induction machine in this period).

[4] This mode is similar to regenerative breaking in induction machines the principal difference being that the BDFRM operation can be sustained.

[5] Switching ripples are present on the secondary waveforms but are generally of very low magnitude (in relative sense) if a small inverter is used. They are virtually non-existent on the primary side because of the inherently weak magnetic coupling between the windings.

However, when controlled, the BDFRM torque and speed waveforms accurately follow the desired trajectories (in this operating region the BDFRM is similar to an adjustable speed synchronous machine). Notice that the electromagnetic torque values in steady-state for the unloaded machine are well above zero since the iron losses have not been accounted for in the control model.

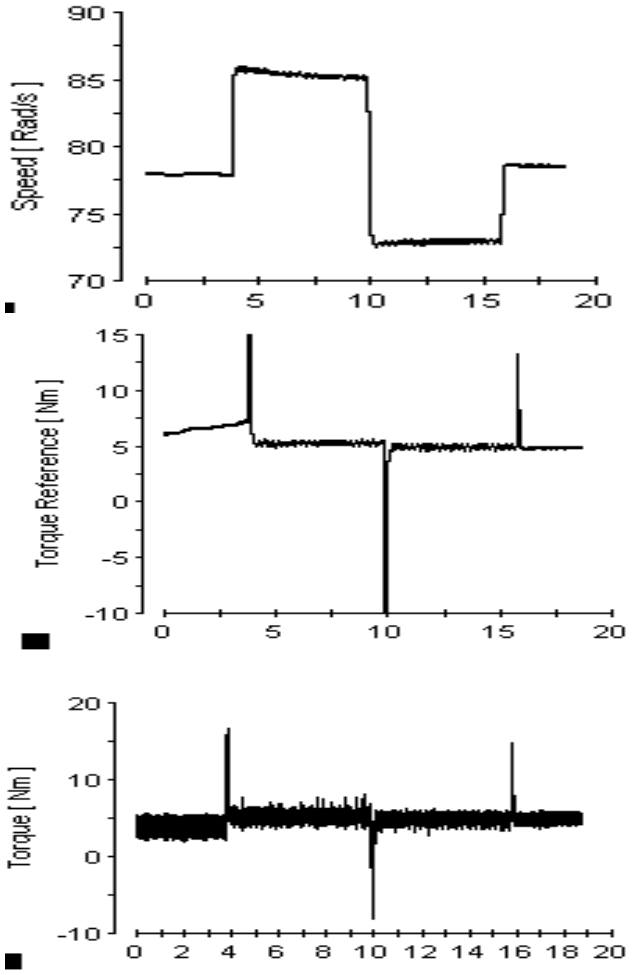

Figure 6: Experimental waveforms from dSPACE

6 Conclusions

The fundamental principles and performance analysis of different control techniques for the BDFRM have been presented in the paper. This kind of unified approach can be extremely useful for research and control development of the BDFRM, especially for limited variable speed range applications, such as large pumps or off-shore wind energy conversion systems, where the machine may potentially find its wider use as a low cost, reliable and maintenance-free brushless candidate. The focus of the work has been on the scalar control and particularly on the DTC as these two control methods have been least studied in the available BDFRM literature. In this respect, the paper represents a significant contribution to BDFRM knowledge.

References

[1] M.G.Jovanović, R.E.Betz, and J.Yu, "The use of doubly fed reluctance machines for large pumps and wind turbines," *IEEE Transactions on Industry Applications*, vol. 38, pp. 1508–1516, Nov/Dec 2002.

[2] M.G.Jovanović and R.E.Betz, "Power factor control using brushless doubly fed reluctance machines," *Proc. of the IEEE-IAS Annual Meeting*, Rome, Italy, October 2000.

[3] L. Xu, L. Zhen, and E. Kim, "Field-orientation control of a doubly excited brushless reluctance machine," *IEEE Transactions on Industry Applications*, vol. 34, pp. 148–155, Jan/Feb 1998.

[4] F.Wang, F.Zhang, and L.Xu, "Parameter and performance comparison of doubly-fed brushless machine with cage and reluctance rotors," *IEEE Transactions on Industry Applications*, vol. 38, pp. 1237–1243, Sept/Oct 2002.

[5] R.E.Betz and M.G.Jovanović, "The brushless doubly fed reluctance machine and the synchronous reluctance machine - a comparison," *IEEE Transactions on Industry Applications*, vol. 36, pp. 1103–1110, July/August 2000.

[6] M.G.Jovanović, J.Yu, and E.Levi, "Direct torque control of brushless doubly fed reluctance machines," *Electric Power Components and Systems*, vol. 32, pp. 941–958, October 2004.

[7] M.G.Jovanović, J.Yu, and E.Levi, "A direct torque controller for limited speed range applications of brushless doubly-fed reluctance motors," *CD-ROM proc. of IEEE-IAS Annual Meeting*, Seattle,October 2004.

[8] R.E.Betz and M.G.Jovanović, "Introduction to the space vector modelling of the brushless doubly-fed reluctance machine," *Electric Power Components and Systems*, vol. 31, pp. 729–755, August 2003.

[9] I.Takahashi and T.Noguchi, "A new quick-response and high-efficiency control strategy of an induction machine," *IEEE Transactions on Industry Applications*, vol. IA-22, pp. 820–827, Sept/Oct 1986.

[10] P. Vas, *Sensorless Vector and Direct Torque Control*. Oxford University Press, 1998, ISBN 0-19-856465-1.